Table 1 Genetic polymorphism and spatial pattern of differentiation within each population in *Malus sylvestris*. Five genotypes could not be assigned to any population, and thus, analyses were conducted on a total of $N = 376$ individuals

	Population		
	W (red)	NE (green)	SE (blue)
Microsatellite polymorphism			
N	213	90	73
H_O	0.69	0.77	0.80
H_E	0.74	0.85	0.88
F_{IS}	0.07***	0.10***	0.09***
A_r	11.5	15.3	17.3
A_p	1.3	2.1	4.4
Spatial pattern (logarithm)			
Sp	0.005	0.004	−0.003
Mean[Ln(*dist*)]	1.3	1.3	0.8
b	−0.006***	−0.004***	−0.001***
$F_{(1)}$	0.03	0.01	0.02
r^2	0.008	0.008	0.009

8 N: sample size of each population, H_O and H_E: observed and expected heterozygosities, F_{IS}: inbreeding coefficient, A_r: mean allelic richness for loci, corrected by the rarefaction method, estimated for a sample size of 100, A_p: number of private alleles, corrected by the rarefaction method, estimated for a sample size of 100, Sp: Sp parameter, mean[Ln(*dist*)]: mean of the logarithm of the geographical distance between genotypes, b regression slope between F_{ij} and the logarithm of geographical distance, $F_{(1)}$: mean F_{ij} between individuals from the first distance class, r^2: squared correlation coefficient between the logarithm of geographical distance and F_{ij}.
*$0.05 < P \leq 0.01$, **$0.01 < P \leq 0.001$, ***$P < 0.001$.

(model *b*) gene flow, (ii) divergence and expansion of the W and SE populations, followed by the divergence and expansion of the NE population derived from the SE population (i.e. resulting from a more recent colonization wave front), with (model *c*) or without (model *d*) gene flow (Fig. 1). The correlations between model parameters and summary statistics are presented in Fig. S6 (Supporting information). The relative posterior probabilities calculated for each model provided the strongest statistical support for model *a*, suggesting that the three populations (W, SE and NE) diverged simultaneously, with all populations growing exponentially and bidirectional gene flow occurring between each pair of populations during expansion (Table 2; Bayes factor for model $a = 4.37$). The models with the NE population diverging from the SE population (models *c* and *d*) had the lowest relative posterior probabilities (Table 2). The migration rates per generation were estimated at $m_{W\text{-}SE} = 0.01$ [95% HPD: 0–0.21], $m_{W\text{-}NE} = 0.03$ [0–0.21], $m_{SE\text{-}NE} = 0.01$ [0–0.22], $m_{SE\text{-}W} = 1.01 \times 10^{-15}$ [0–0.17], $m_{NE\text{-}SE} = 1.01 \times 10^{-15}$ [0–0.21] and $m_{NE\text{-}W} = 0.05$ [0–0.27]. We obtained estimates of effective population sizes of 40 883 [524–828 327] for N_W, 20 691 [505–565 916] for N_{NE} and 40 882 [524–828 327] for N_{SE}. Using a generation time of 7.5 years, we estimated the population split to have occurred 303 016 years ago [120 963–545 649] (Fig. S7, Supporting information).

We also checked that the power of the analysis was sufficiently high to discriminate between the competing models: for model *a* against all three other models, the type I error rate and the mean type II error rate were 0. Overall, ABC analyses provided clear strong support

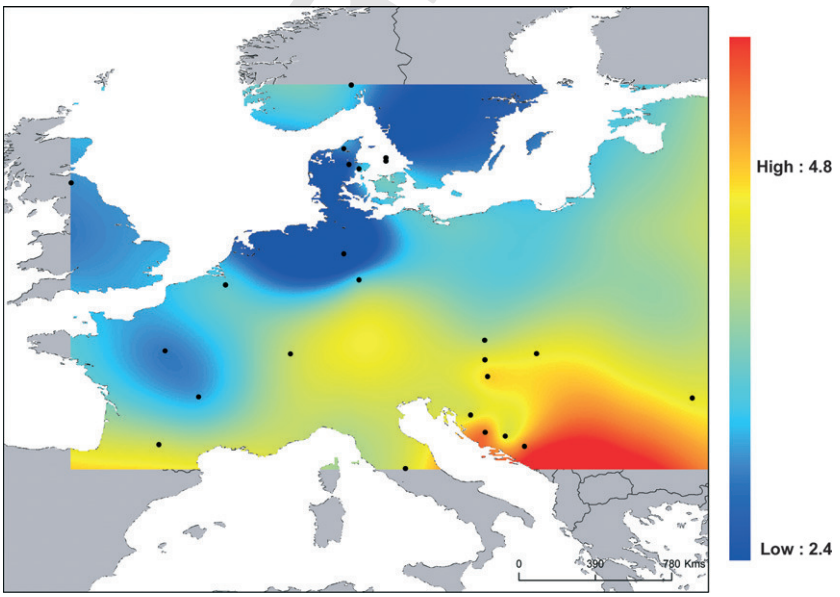

Fig. 4 Map of overall allelic richness (22 sites).

COLOR